N O T I C E

THIS DOCUMENT HAS BEEN REPRODUCED FROM MICROFICHE. ALTHOUGH IT IS RECOGNIZED THAT CERTAIN PORTIONS ARE ILLEGIBLE, IT IS BEING RELEASED IN THE INTEREST OF MAKING AVAILABLE AS MUCH INFORMATION AS POSSIBLE

NI

NASA Technical Memorandum 81589

Solution of Plane Cascade Flow Using Improved Surface Singularity Methods

Eric R. McFarland
Lewis Research Center
Cleveland, Ohio

Prepared for the
Twenty-sixth Annual International Gas Turbine Conference
sponsored by the American Society of Mechanical Engineers
Houston, Texas, March 8-12, 1981

NASA

SOLUTION OF PLANE CASCADE FLOW USING IMPROVED SURFACE SINGULARITY METHODS

by Eric R. McFarland

NASA Lewis Research Center
Cleveland, Ohio

ABSTRACT

A solution method has been developed for calculating compressible inviscid flow through a linear cascade of arbitrary blade shapes. The method uses advanced surface singularity formulations which were adapted from those found in current external flow analyses. The resulting solution technique provides a fast flexible calculation for flows through turbomachinery blade rows. The solution method and some examples of the method's capabilities are presented.

NOMENCLATURE

As, Bs, Av, Bv, Ad, Bd	source, vortex, and vortex jump influence coefficients
C	blade chord
c	curvature parameter
$\bar{i}, \bar{j}$	unit vectors
f	a control point on the cascade surface
$\bar{n}, \bar{t}$	surface unit normal and tangential vectors
P	arbitrary point in space
S	cascade pitch or gap
s	surface distance from center of panel
V	velocity relative to the blade
v	disturbance velocity
X, Y	$\pi(x - \xi)/S$, $\pi(y - \eta)/S$
x, y	coordinate system associated with the point where the velocity is to be calculated
α	flow angle relative to axial direction
β	cascade stagger or blade setting angle
Δ	element or panel chord length
ξ, η	coordinate system associated with cascade elements
σ, γ, δ	source, vortex, and vortex jump singularity strengths
Φ	total velocity potential
ϕ	component of total velocity potential
θ	orientation angle of panel or velocity point coordinate system with respect to reference coordinate system
ρ	fluid density
∇	gradient vector operator

Subscripts:

i, c	incompressible and compressible
E, I	exit and inlet conditions
i, j, k	panel indices for source, vortex, and vortex jump singularity strengths
N, T	normal and tangential component on blade surfaces
TE	trailing edge quantity
t	stagnation or total condition
U, L	upper and lower surfaces
onset	mean undistrubed flow

Overbars:

$\bar{(\ )}$	vector quantity
$\tilde{(\ )}$	averaged quantity

INTRODUCTION

Current design of turbomachinery blade rows relies on the use of computer codes to model the flow on blade-to-blade surfaces. Most of the codes currently used for blade designs model the flow as inviscid, irrotational and compressible. The flow field is solved using finite difference or finite element numerical techniques. The solutions given by these codes can be quite accurate. However, it has been the experience of the author that use of the field techniques can require an experienced user to manipulate input data and control parameters, and that these codes may also limit a designer in the types of blade geometries, cascade configurations, and flow conditions that can be considered. The designer can therefore spend a considerable portion of his effort in making a preliminary design conform to the requirements and eccentricities of a particular flow analysis code. In order to accelerate the blade design process and give the designer more freedom in developing blade shapes, a simple blade-to-blade flow code has been developed. The objective of the code is to provide a versatile, stable, and efficient calculation which has sufficient accuracy to determine the basic merits of a particular blade row design. The simple code provides a means of rapidly screening blade designs for analysis by more complex codes which have better accuracy.

The panel or integral equation solution technique was selected as a basis for the simple design code. This technique meets the requirements of being a versatile, stable, and efficient calculation scheme. It is however an incompressible solution and requires the use of a compressibility correction to account for compressible flow effects.

Panel solutions have been used for several years by external aerodynamicists who have developed and refined them into one of the primary design tools of the aircraft industry. In the past, internal flow aerodynamicists such as Martensen [1], Geising [2], and Hess and Stockman [3] have made use of integral solutions, but the basic technique has not been pursued extensively for internal flow problems.

In this paper a panel solution is described for inviscid compressible flow through a plane cascade. An incompressible solution is developed using advanced integral equation formulations. Compressibility effects and stream channel variatons are included by adapting the Lieblein-Stockman correction technique [4] from engine inlet calculations to the cascade problem. Several example solutions are given to demonstrate the capabilities of the method.

ANALYSIS

The general cascade problem is shown in figure 1. The governing equations and boundary conditions for an inviscid incompressible cascade flow are the following:

$$\nabla \cdot \bar{V} = 0 \tag{1}$$

$$P + \frac{1}{2}\rho V^2 = \text{constant} = P_t \tag{2}$$

$$\bar{V} \cdot \bar{n}_{\substack{\text{body} \\ \text{surface}}} = \bar{V}_{N_{\substack{\text{body} \\ \text{surface}}}} \tag{3}$$

$$\bar{V} \to \bar{V}_1 \quad \text{as} \quad x \to -\infty \tag{4}$$

$$\bar{V} \to \bar{V}_2 \quad \text{as} \quad x \to +\infty \tag{5}$$

The solution is developed using a velocity potential which is the sum of a constant velocity potential plus a disturbance. The constant velocity potential is determined from the mean of the upstream and downstream velocities. The disturbance quantities are unknown.

$$\phi = \phi_{onset} + \phi$$

$$\bar{V} = -\nabla\phi = \bar{V}_{onset} + \bar{v} \tag{6}$$

The constant or onset velocity and potential satisfy continuity (eq. (1)) exactly. The disturbance potential and velocity are to be determined so that continuity is satisfied.

$$\nabla \cdot \bar{v} = \nabla^2\phi = 0 \tag{7}$$

$$\bar{V}_{onset} = \text{constant} \tag{8}$$

The flow field is determined by solving equations (6), (7), and (8) subject to boundary conditions (3), (4), and (5). The momentum equation (2) does not enter into the calculation except to relate the pressure to the velocity field.

The equation for the disturbance potential (eq. (7)) is Laplace's equation. Since it is a linear equation, superposition of known simple solutions of Laplace's equation may be used to develop more complex solutions. A general solution to flow over a body or cascade of bodies may be developed by using basic incompressible potential flow solutions for source and vortex flows distributed along the body surfaces, and varying the strength of the source and vortex singularities so that the problem's boundary conditions are satisfied. This is the basis of the panel method as described by Hess and Smith [5].

In practice the surface of the body is represented by inscribing a polygon as shown in figure 2. The simple source and vortex singularity solutions are described over each element, and a control point is selected on each element where the normal velocity boundary condition is to be applied. There will be n element end points and $n-1$ control points. The first and n^{th} element end points are coincident.

The simplest form of the solution would be to use flat elements with constant source and vortex sinularity strengths over each element and the control points located at the center of the flat element. However, Hess [6] demonstrated a means of developing higher order accurate panel solutions by using curved elements with varying singularity strengths and locating the control points closer to the true body surface. Building on Hess's work, a higher order accurate panel solution is developed for linear cascades.

Cascade panel formulation. A single cascade panel is shown in figure 3. The panel has associated with it a cartesian coordinate system with unit vectors $\bar{i},\bar{j}$. The coordinate system is centered on the panel. Its origin is located at the panel control point and the x or ξ axis is aligned with the panel chord. The velocity at any point P due to the singularity distribution along each cascade panel is to be determined. The coordinates for point P are denoted as x,y and those for points on the panel as ξ,η.

Hess showed that the velocity at any point P due to a single panel with a source strength distribution, $\sigma(s)$, is given by

$$\bar{V} = 2\int_{-\Delta/2}^{\Delta/2}\left[\frac{x-\xi}{r^2}\bar{i} + \frac{y-\eta}{r^2}\bar{j}\right]\sigma(s)\frac{ds}{d\xi}\,d\xi \qquad (9)$$

where

$$r = \sqrt{(x-\xi)^2 + (y-\eta)^2}$$

For a cascade problem a series of these integrals is needed.

$$\bar{V} = 2\int_{-\Delta/2}^{\Delta/2}\left[\frac{(x-\xi)\bar{i} + (y-\eta)\bar{i}}{r^2}\right.$$

$$+\sum_{k=1}^{\infty}\left\{\frac{(x-\xi)\bar{i} + (y-(\eta-kS))\bar{j}}{(x-\xi)^2 + (y-(\eta-kS))^2}\right.$$

$$\left.\left.+\frac{(x-\xi)\bar{i} + (y-(\eta+kS))\bar{j}}{(x-\xi)^2 + (y-(\eta+kS))^2}\right\}\right]\sigma(s)\frac{ds}{d\xi}\,d\xi \qquad (10)$$

where k is the summation index for cascade bodies. This series is the cascade potential velocity which was shown in reference 2 to be

$$\bar{V} = \frac{2\pi}{S}\int_{-\Delta/2}^{\Delta/2}\left[\frac{\sinh(X)\cosh(X)\bar{i} + \sin(Y)\cos(Y)\bar{j}}{\sinh^2(X) + \sin^2(Y)}\right]\sigma(s)\frac{ds}{d\xi}\,d\xi \qquad (11)$$

where

$$X = \frac{\pi}{S}(x-\xi);\quad Y = \frac{\pi}{S}(y-\eta)$$

Hess [6] developed the higher order panel formulas by integrating equation (9) using series expansions for the different terms in the integrand. These expansions for a second order accurate panel solution are

$$\eta = c\xi^2 + O(\xi^3)$$

$$\sigma = \sigma_0 + \sigma_1 s + O(s^2)$$

$$s = \xi + \frac{2}{3}c^2\xi^2 + O(\xi^4)$$

$$\frac{1}{r^2} = \frac{1}{r_f^2} + \frac{2cy\xi^2}{r_f^4} + O(\xi^4) \qquad (12)$$

where

$$r_f = \sqrt{(x-\xi)^2 + y^2}$$

The factor c appearing in the series expansion is related to the panel curvature and is determined by a three point curve fit using the averaged element slopes at the end points of the panel. The expansion of $1/r^2$ is needed for numerical stability. As point P approaches the path of integration the integrand becomes very large and the resulting expression for velocity becomes divergent. The expansion in terms of r_f alleviates this problem.

In the present study equation (11) was integrated numerically. The series expansions for η,s,σ in terms of ξ were substituted into the integrand. The resulting expression was evaluated using a three point ($\xi = -\Delta/2, 0, \Delta/2$) Simpson's rule. Again, numerical difficulties were encountered in calculating the integrands as the velocity point approached the path of integration. However, from equation (10) it can be seen that only the first term in the series is causing the difficulty and that this term is identical to the velocity equation for an isolated body (eq. (9)). Therefore, the numerical problem may be avoided by subtracting the first term of the series from the integrand, integrating, and adding Hess's analytical expression to the integral. Equation (11) becomes

$$\bar{V} = \frac{2\pi}{S}\int_{-\Delta/2}^{\Delta/2}\left[\frac{\sinh(X)\cosh(X)\bar{i} + \sin(Y)\cos(Y)\bar{j}}{\sinh^2(X) + \sin^2(Y)}\right.$$

$$\left.-\left\{\frac{X\bar{i} + Y\bar{j}}{X^2 + Y^2}\right\}\right](\sigma_0 + \sigma_1\xi)(1)d\xi + \bar{V}_{\substack{\text{isolated}\\ \text{body}}} \qquad (13a)$$

Equation (13a) has been developed for a source singularity distribution. It can also be used for the vortex singularity distribution since from incompressible potential flow theory the source and vortex singularities are related. The vortex equation would be similar to equation (13a) except σ would be replaced by γ, the velocity components change. The resulting equation is

$$\bar{V} = \frac{2\pi}{S}\int_{-\Delta/2}^{\Delta/2}\left[\frac{\sin(Y)\cos(Y)\bar{i} - \sinh(X)\cosh(X)\bar{j}}{\sinh^2(X) + \sin^2(Y)}\right.$$

$$\left.-\left\{\frac{Y\bar{i} - X\bar{j}}{X^2 + Y^2}\right\}\right](\gamma_0 + \gamma_1\xi)(1)d\xi$$

$$+2\int_{-\Delta/2}^{\Delta/2}\left[\frac{(y-\eta)\bar{i} - (x-\xi)\bar{j}}{r^2}\right]\gamma(s)\frac{ds}{d\xi}\,d\xi \qquad (13b)$$

Integral equation formulation. The integral equation formulation of Bristow [7] was used in the present cascade panel solution. The primary feature of this formulation is the use of Green's third identity [8]. Bristow demonstrated that by using this identity for two dimensional flow a direct relationship can be developed between the onset flow, and the source and vortex singularity distributions. Along the body surface the tangential and normal velocity will be given by

$$V_T = V_{onset} \cdot \bar{t} + \gamma \tag{14a}$$

$$V_N = V_{onset} \cdot \bar{n} + \sigma \tag{14b}$$

These relationships mean that the singularity strengths will remain bounded regardless of the flow boundary conditions or geometry. Bristow [7] showed that the mild singularity strength distribution generated by using Green's third identity will result in panel solutions which are less sensitive to coordinate smoothness and thin airfoil geometries.

Before making use of Green's third identity, an approximation of equation (6) is needed. This can be written in scalar components as

$$V_{x_p} = V_{onset} \cos(\theta_p - \alpha) + \sum_{i=1}^{n-1} As_{pi}\sigma_i + \sum_{j=1}^{n} Av_{pj}\gamma_j + \sum_{k=1}^{m} Ad_{pk}\delta_k \tag{15a}$$

$$V_{y_p} = - V_{onset} \sin(\theta_p - \alpha) + \sum_{i=1}^{n-1} Bs_{pi}\sigma_i + \sum_{j=1}^{n} Bv_{pj}\gamma_j + \sum_{k=1}^{m} Bd_{pk}\delta_k \tag{15b}$$

The first terms in the equations (15) are the contribution of the constant or onset velocity to the total velocity vector in equation (6). The angles θ and α are the orientations of the coordinate system associated with point P and the onset velocity vector with respect to a reference direction. The summation terms represent the disturbance velocity v in equation (6). Each term in the summation is an integration of equations (13a) or (13b) over one of the elements which make up the cascade body. The A's and B's in the summations are coefficients of the singularity strength values from the element integrations. These influence coefficients depend on the geometry of the problem and must be recalculated for each point where a velocity calculation is to be made. The source strengths σ which are assumed to vary linearly over the element surface are defined in terms of the element control points using a three point curve fit. The vortex strengths γ also are assumed to vary linearly, but they are defined in terms of the element end points using four point divided differences. The additional singularity strengths δ are part of the vortex singularity distribution. They represent a jump in the vortex strength which Green's identity, equation (14a), indicates will occur at discontinuities in surface slopes. Such discontinuities are encountered for example at sharp leading and trailing edges of blades. When a surface slope discontinuity is encountered in the calculation, one sided curve fits and differences are used for the source, vortex, and geometry terms on each side of the discontinuity.

Normalizing equations (14) and (15) by the onset velocity magnitude, applying equation (15) to a control point ℓ on the body surface, and resolving the calculated velocity into tangential and normal velocity components, expressions for the surface velocity may be written which relate Green's third identity to the integral equation approximation.

$$V_{T_\ell} = \cos(\theta_\ell - \alpha) + \gamma_\ell^* \tag{16a}$$

$$V_{N_\ell} = - \sin(\theta_\ell - \alpha) + \sigma_\ell \tag{16b}$$

$$V_{T_\ell} = \cos(\theta_\ell - \alpha) + \sum_{i=1}^{n} As_{\ell i}\sigma_i + \sum_{j=1}^{n-1} Av_{\ell j}\gamma_j + \sum_{k=1}^{m} Ad_{\ell k}\delta_\ell \tag{16c}$$

$$V_{N_\ell} = - \sin(\theta_\ell - \alpha) + \sum_{i=1}^{n} Bs_{\ell i}\sigma_i + \sum_{j=1}^{n-1} Bv_{\ell j}\gamma_j + \sum_{k=1}^{m} Bd_{\ell k}\delta_\ell \tag{16d}$$

where γ with an * denotes that the vortex strength is evaluated at a panel control point while γ without an * is evaluated at the panel end point.

A system of linear algebraic equations to calculate the singularity strengths may now be constructed. This system of equations is similar to those developed by Bristow [7] for isolated bodies. These equations are generated by using the normal velocity surface boundary condition, farstream boundary conditions, and a tangential velocity error minimization equation. The normal velocity boundary condition is first used with equation (16b) to solve for the source strengths, and then with equation (16d) to give n - 1 equations. The farstream boundary conditions, the given inlet and exit flow angles, are used to calculate the circulation of the cascade. This is used with equation (16c) to provide one equation. The tangential velocity error minimization equations are needed if there are surface slope discontinuities, and vortex jump strengths are to be calculated. One minimization equation will be added to the system for each surface slope discontinuity. The tangential velocity error function is the sum of the squares of the difference between equations (16a) and (16c) multiplied by the local panel chord length.

This system of equations satisfies all the problem boundary conditions and includes all the unknown singularity strengths. However, there is one more equation than unknowns. This occurs because the first and last element end points are coincident for a closed body and therefore γ_1 and γ_n are equal. The additional unknown used to complete the system is an assumed uniform error in the normal velocity boundary conditions. The uniform error variable is denoted as ε and is included in the normal velocity equations.

In final form the equations to be solved for the singularity strengths and uniform error are:

1. Normal velocity surface boundary condition

$$\sigma_i = \sin(\theta_i - \alpha) + V_{N_i} \tag{17a}$$

$$\sum_{j=1}^{n} Bv_{\ell j}\gamma_j + \varepsilon + \sum_{k=1}^{m} Bd_{\ell k}\delta_k = V_{N_\ell} + \sin(\theta_\ell - \alpha) - \sum_{i=1}^{n-1} Bs_{\ell i}\sigma_i$$

2. Circulation

$$\Gamma = S \cos(\alpha)\left[\tan(\alpha_1) - \tan(\alpha_2)\right] \tag{17b}$$

$$+ \oint_{body} V_T ds \tag{17c}$$

$$\sum_{\ell=1}^{n-1}\left(\sum_{j=1}^{n} Av_{\ell j}\gamma_j + \sum_{k=1}^{m} Ad_{\ell k}\delta_k\right)\Delta_\ell = \Gamma$$

$$- \sum_{\ell=1}^{n-1}\left(\cos(\theta_\ell - \alpha) + \sum_{i=1}^{n-1} As_{\ell i}\sigma_i\right)\Delta_\ell \qquad (17d)$$

3. Tangential error minimization

$$\frac{\partial}{\partial\delta_\ell}\left\{\sum_{i=1}^{n-1}\left(V_{T_{16c}} - V_{T_{16a}}\right)_i^2 \Delta_i\right\} = 0$$

$$\sum_{j=1}^{n}\left[\sum_{i=1}^{n-1}\left(\Delta_i Ad_{i\ell} Av_{ij}\right) - \left(\Delta_j Ad_{j\ell} + \Delta_{j-1} Ad_{j-1\ell}\right)/2\right]\gamma_j$$

$$+ \sum_{k=1}^{m}\left[\sum_{i=1}^{n-1} \Delta_i Ad_{i\ell} Ad_{ik}\right]\delta_k = - \sum_{j=1}^{n-1}\left[\sum_{i=1}^{n-1} \Delta_i Ad_{i\ell} As_{ij}\right]\sigma_j \qquad (17e)$$

If only the upstream flow conditions are given, the circulation cannot be calculated directly and equation (17d) is replaced by a Kutta condition. An iteration procedure is then used to find the proper onset flow direction and circulation. The Kutta condition for sharp trailing edges is the same as Bristow [7] used, that is, flow normal to the trailing edge bisector is zero. For the round trailing edge found in turbomachinery, this condition is modified. Two-line segments are constructed parallel to the trailing edge bisector from the trailing edge circle tangency points of the upper and lower blade surfaces. At a point on each line just downstream of the trailing edge, the normal flows to these lines are required to be equal and opposite. The two types of Kutta conditions are illustrated in figure 4. The Kutta condition equation is written as

$$\sum_{j=1}^{n}\left(Bv_{TE,U} + Bv_{TE,L}\right)_j \gamma_j + 2\epsilon = 2\sin(\theta_{TE} - \alpha)$$

$$- \sum_{i=1}^{n-1}\left(Bs_{TE,U} + Bs_{TE,L}\right)_i \sigma_i \qquad (18)$$

In the iteration procedure equations (17a), (17b), (18), and (17e) are solved using a guessed value for α. The resulting singularity strengths are used in equation (17d) to determine the circulation. The calculated circulation and onset flow angle α are then used in the following relation to determine the upstream flow condition

$$\alpha_I = \tan^{-1}\left[\frac{\sin(\alpha) + \Gamma/(2S)}{\cos(\alpha)}\right] \qquad (19)$$

If the calculated value of α_I differs from the specified inlet value, the onset flow angle α is updated and the procedure is repeated.

This system of equations is solved using a direct method. The technique used is known as Cholesky's method. It resolves the coefficient matrix into upper and lower triangular matrices so that additional solutions for variations in surface normal velocities and farstream boundary conditions require only a back substitution. This property is used in the iteration procedure for the Kutta condition and in the calculation of multiple inlet and exit flow angle cases.

Compressibility correction. The internal flow compressibility correction of Lieblein and Stockman [4] is used in this study. This correction has been used successfully for a number of years to calculate engine inlet flows. The correction is expressed in the following form

$$V_c = V_i\left(\rho_i/\tilde{\rho}_c\right)^{V_i/\tilde{V}_i} \qquad (20)$$

where V_c is the corrected compressible velocity, V_i is the local incompressible velocity from the panel solution, ρ_i is the incompressible density taken to be the stagnation density ρ_t, $\tilde{\rho}_c$ is the average compressible density, and $\tilde{V}_i$ is the average incompressible velocity across the flow passage. The average compressible density is found by solving the following expression derived from the one-dimensional continuity equation and the isentropic relations.

$$\left(\frac{\tilde{\rho}_c}{\rho_t}\right)\left\{\frac{\gamma+1}{\gamma-1}\left[1 - \left(\frac{\tilde{\rho}_c}{\rho_t}\right)^{\gamma-1}\right]\right\}^{1/2} = \frac{\tilde{V}_i}{V_{cr}}$$

where γ is the ratio of specific heats and V_{cr} is the critical velocity. The average incompressible velocity is calculated on planes which are normal to the mean flow and which contain the local velocity to be corrected.

For inlets with little streamwise turning of the flow, the application of the compressibility correction is straightforward. The mean flow direction can be assumed to be approximately normal to axial stations and the average incompressible velocities are calculated using the axial station flow areas. However, for cascade flows with significant amounts of flow turning, the mean flow direction cannot be assumed and must be calculated. In this study, the components of the mean velocities are first calculated at axial stations by using continuity and circulation equations. Next the mean flow direction through the blade passage is determined from the axial station velocity components. Planes normal to the mean flow are then constructed for each surface velocity to be corrected. Finally, the average incompressible velocity on the normal planes is found by interpolation of the axial station values.

Stream channel variation corrections. A simple correction for given stream channel variations is made during the compressibility correction calculation. The incompressible surface velocities and mean flow are calculated assuming a uniform stream channel height using the inlet flow conditions as a reference. These velocities are then scaled by the ratio of the inlet to local specified stream channel height. The resulting scaled velocities are used in the compressible corrections of equation (20).

SAMPLE CALCULATIONS AND DISCUSSION

Four sample calculations are presented to demonstrate the solution method. Table I shows the general flow and solution conditions for each calculation. All examples were calculated using the IBM 3033 computer at Lewis Research Center. A FORTRAN computer code of the solution method was developed for the calculations. Most blade shapes were approximated by using 40 to 60 elements and the solution required less than 4 seconds of computer time. While this computation time is very rapid, it should be noted that compressible field methods have been reported which have run times on the same order [9]. In the Gostelow and Sanz cases, the cascade airfoil shapes were described directly using discrete points. However, in the Katsanis and Hobson cases, the cascade body shapes were generated by using spline fits for the upper and lower surfaces, and circles or ellipses for the rounded leading and trailing edges.

Incompressible cascade flow. The exact incompressible solution of Gostelow [10] is compared with the present solution in figure 5. The large velocity gradients in the leading edge region and the flow past the thin trailing edge are well modeled by the panel solution. The overall agreement between the two solutions is very good.

Compressible cascade flow. In figure 6 a comparison is shown between the panel solution and the finite difference solution of Katsanis [11] for a turbine stator. Blade surface velocities are in the high subsonic range. The overall solution agreement is good, but differences do occur along the pressure surface and near the suction surface trailing edge. These differences are attributable to the compressibility correction, since the two solutions were found to be identical for incompressible flow through the same cascade.

The general accuracy of the panel method is also shown in figure 6. Two panel solutions are shown with a different number of panels used in each case. The less accurate solution with fewer panels differs slightly from the more accurate solution. Most of this difference occurs in the leading edge region where large variations in surface curvature occur. The coarser paneling is unable to resolve the rapid change in curvature and as a result the curvature effect on the flow is smeared over a larger surface area. By considering the terms used in developing the cascade panel solution, the accuracy of the solution should be on the order of the panel size squared; although this accuracy has not been verified.

Transonic cascade flow. Comparisons with transonic hodograph solutions are shown in figures 7 and 8. In figure 7 the comparison is with Hobson solution [12], and in figure 8 the comparison is with a Sanz cascade blade design using the hodograph solution technique of Bauer, Garabedian, and Korn [13]. The panel solution compares well with the hodograph solutions for the sophistication of the computation involved.

Descrepancies in the solutions are caused primarily by the compressibility correction which cannot be expected to exactly predict the flow at such a high level of compressibility. The large velocity spike at the leading edge of the compressor stator is due to the lack of blade geometry information given in the region, and the extraneous velocities downstream of the blade trailing edge are caused by an extension of the blade downstream to account for the blade wake.

KUTTA CONDITION AND STREAM CHANNEL VARIATION

In the sample calculations just presented, the downstream flow angle was given. These calculations have also been made using the inlet condition and a Kutta condition to determine the downstream flow condition. The calculated downstream flow angles were 31.19° (Gostelow), -67.88° (Katsanis, 32), -67.23° (Katsanis, 98), -44.16° (Hobson), and -31.0° (Sanz). In the first two cases, Gostelow and Katsanis, the flow leaves the blade surface smoothly with little deviation from the trailing edge blade angle and the Kutta condition works well. However, in the Hobson and Sanz cases there is significant flow deviation at the blade trailing edge and the Kutta condition results are poor. Some improvements in these results could be made by including a deviation model in the Kutta condition formulation.

The effect of stream channel variation on the flow has not been studied extensively. Some comparisons have been made with the finite difference code of Katsanis [11] for subsonic flows and the agreement was good.

CONCLUSION

Current external aerodynamic integral equation techniques may be adopted for use in internal flow calculations. The inherent computational speed and flexibility of integral equation solution can make them very useful for design calculations. The present cascade method is a versatile design tool that will allow a designer to explore many preliminary blade designs in a short period of time. Although the method does not give exact solutions for compressible flows, example calculations do demonstrate that it is sufficiently accurate to provide a means of selecting blade designs for further analysis.

REFERENCES

1. Martensen, E., "The Calculation of Pressure Distribution on a Cascade of Thick Airfoils by Means of Fredholm Integral Equations of the Second Kind," NASA TT F-702, 1971.
2. Giesing, J. P., "Extension of the Douglas Neuman Program to Problems of Lifting Infinite Cascades," LB-31653, Douglas Aircraft Co., Inc., Long Beach, CA, 1964. (AD-605207.)
3. Hess, J. L. and Stockman, N. O., "An Efficient User-Oriented Method for Calculating Compressible Flow About Three-Dimensional Inlets," AIAA Paper No. 79-0081, Jan. 1979.
4. Lieblein, S. and Stockman, N. O., "Compressibility Correction for Internal Flow Solutions," Journal of Aircraft. Vol. 9, No. 4, Apr. 1972, pp. 312-313.
5. Hess, J. L. and Smith, A. M. O., "Calculation of Potential Flow About Arbitrary Bodies," Progress in Aeronautical Sciences. Vol. 8, K. Kuchemann, ed., Pergamon Press, Ltd., Oxford, 1967, pp. 1-138.

6. Hess, J. L., "Higher Order Numerical Solution of the Integral Equation for the Two-Dimensional Neumann Problem," Computer Methods in Applied Mechanics and Engineering. Vol. 2, Feb. 1973.
7. Bristow, D. R., "Recent Improvements in Surface Singularity Methods for Flow Field Analysis About Two-Dimensional Airfoils," AIAA paper 77-641, in Computational Fluid Dynamics Conference, 3rd, American Institute of Aeronautics and Astronautics, Inc., New York, 1977, paper no. 77-641, pp. 95-105.
8. Karamcheti, K., Principles of Ideal-Fluid Aerodynamics, Wiley, New York, 1966, pp. 344-350.
9. Caspar, J. R., Hobbs, D. E., and Davis, R. L., "Calculation of Two-Dimensional Potential Cascade Flow Using Finite Area Methods," AIAA Journal, Vol. 18, No. 1, Jan. 1980, pp. 103-109.
10. Gostelow, J. P., "Potential Flow Through Cascades - A Comparison Between Exact and Approximate Solutions," CP No. 807, Aeronautical Research Council, 1963.
11. Katsanis, T., "Fortran Program for Calculating Transonic Velocities on a Blade to Blade Stream Surface of a Turbomachine," NASA TN D-5427, 1969.
12. Hobson, D. G., "Shock-Free Transonic Flow in Turbomachinery Cascades," CUED/A TURBO/TR65, University of Cambridge, Dept. of Eng., 1974.
13. Bauer, F., Garabedian, P., and Korn, D., "Supercritical Wing Sections III," Lecture Notes in Economics and Mathematical Systems, Vol. 150, Springer-Verlag, New York, 1977.

TABLE I. - SAMPLE CALCULATIONS

Case	Inlet		Exit		Gap / Chord	Number of panels	CPU sec IBM TSS/370
	V/V_{cr}	α_I	V/V_{cr}	α_E			
Gostelow	-----	53.5	-----	30.025	1.239	49	2.42
Katsanis	0.231	0	0.727	-67.00	0.747	32/98	1.54/7.30
Hobson	0.610	46.123	0.610	-46.123	0.526	61	3.43
Sanz	0.826	44.61	0.529	3.91	0.863	51	2.61

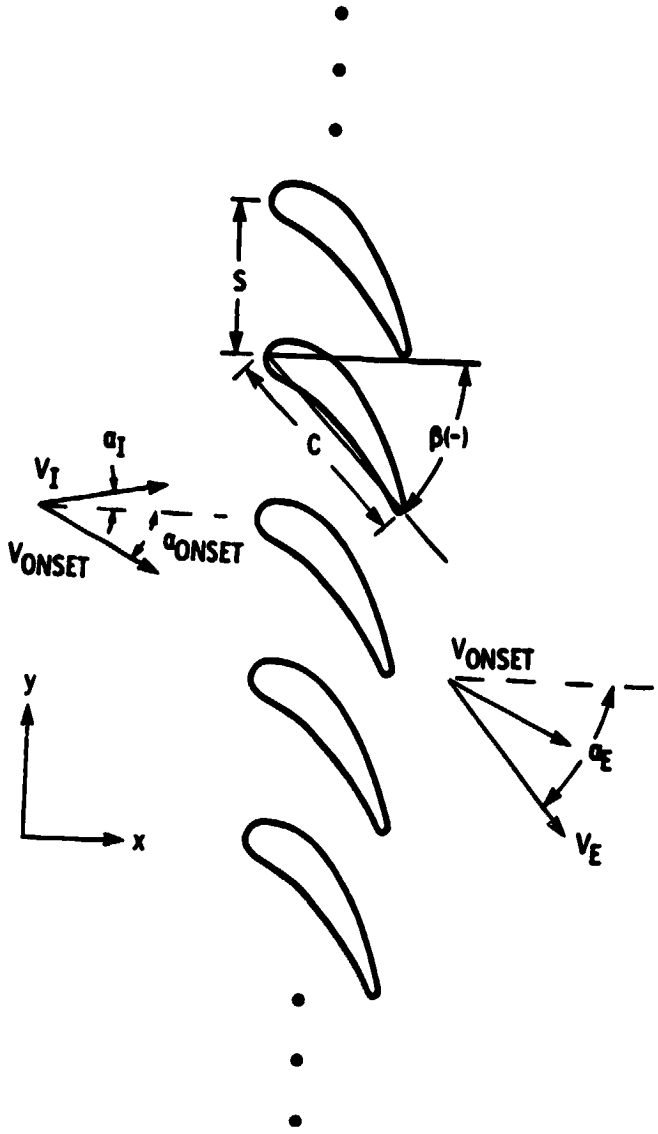

Figure 1. - Cascade problem.

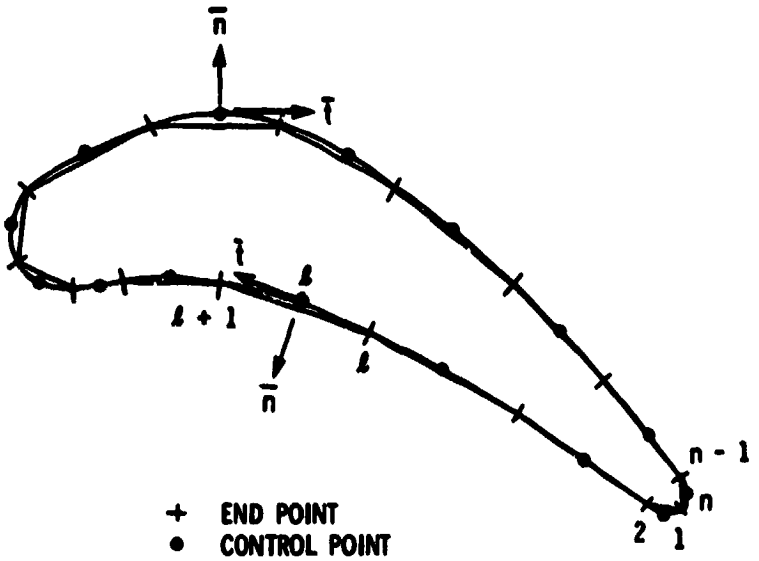

Figure 2. - Panel representation of turbomachinery blade.

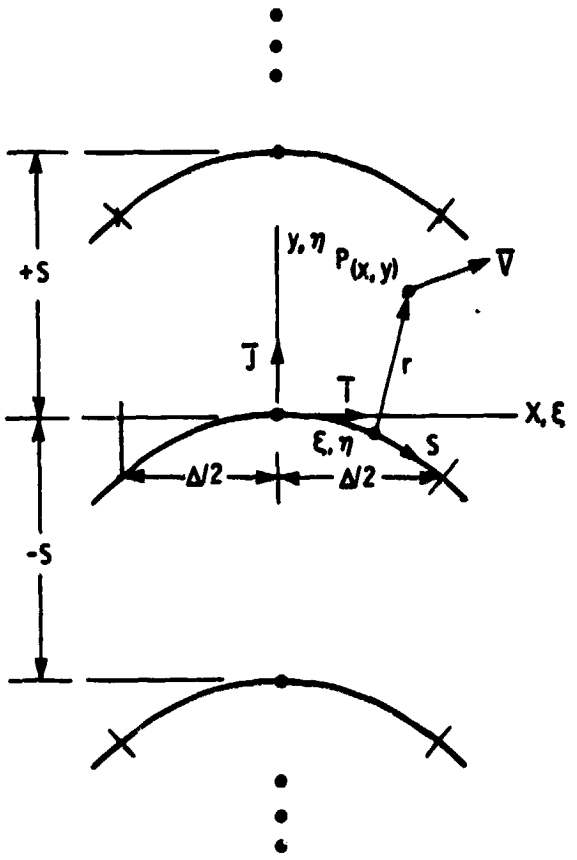

Figure 3. - Cascade panel elements.

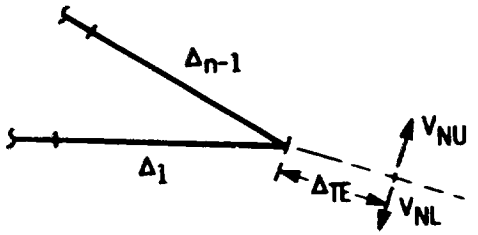

$$\Delta_{TE} = 0.001\,(\Delta_1 + \Delta_{n-1})$$

$$\bar{V}_{NL} = -\bar{V}_{NU} = 0$$

a. Sharp trailing edge.

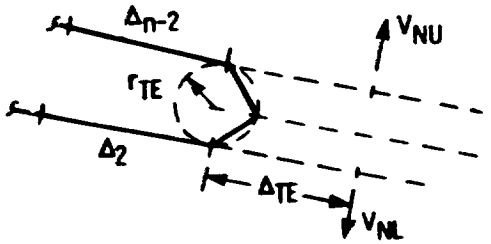

$$\Delta_{TE} = 0.001\,(\Delta_2 + \Delta_{n-2}) + 2r_{TE}$$

$$\bar{V}_{NL} = -\bar{V}_{NU}$$

b. Round trailing edge.

Figure 4. - Kutta condition configurations.

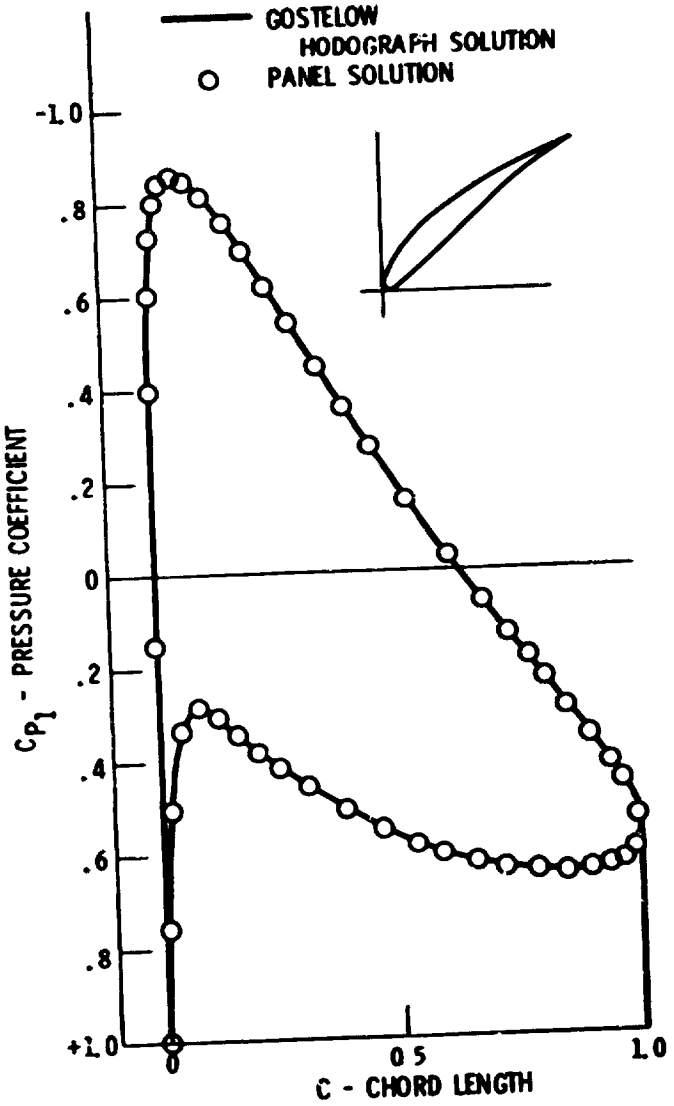

Figure 5. - Incompressible cascade flow.

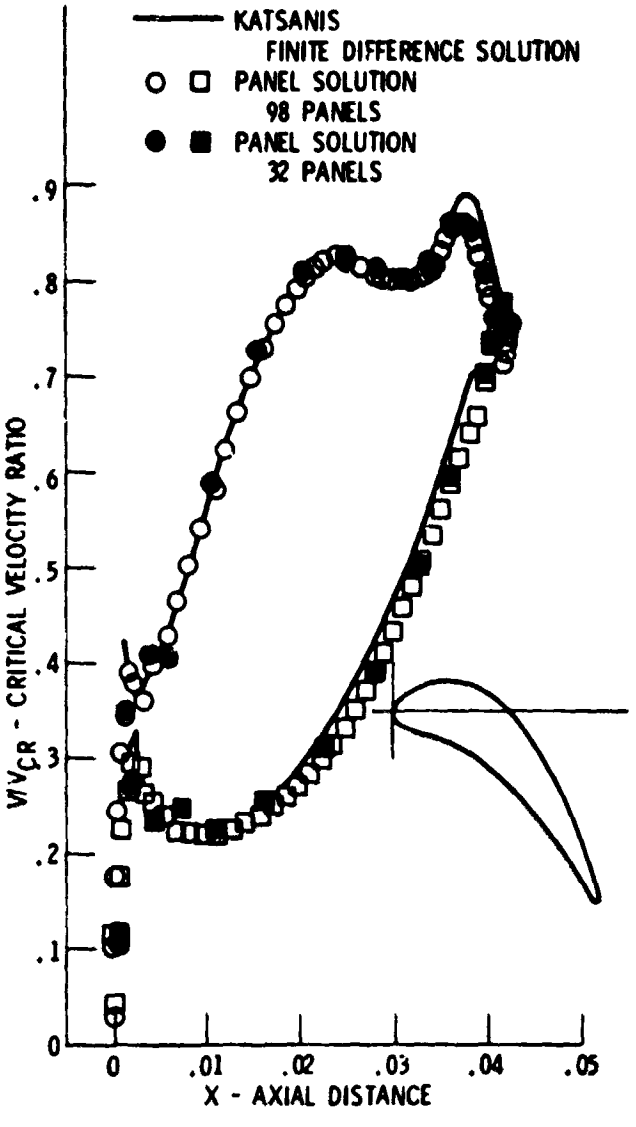

Figure 6. - Compressible cascade flow.

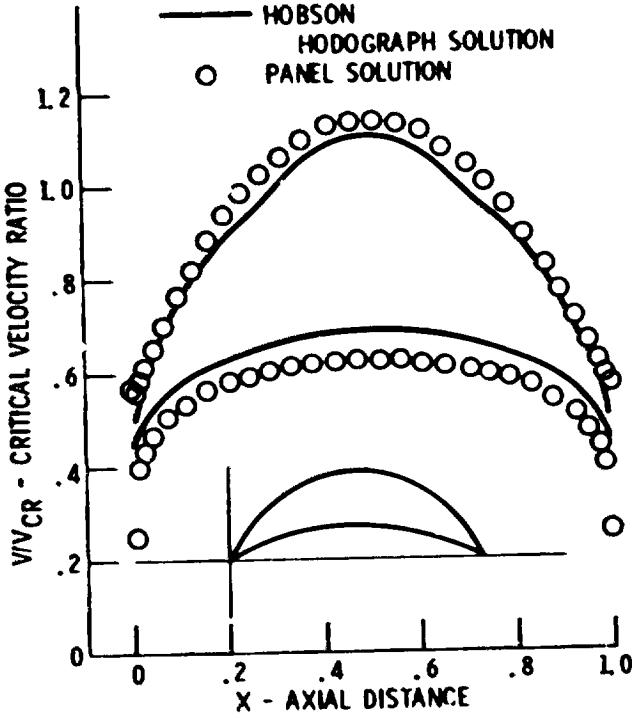

Figure 7. - Transonic cascade flow.

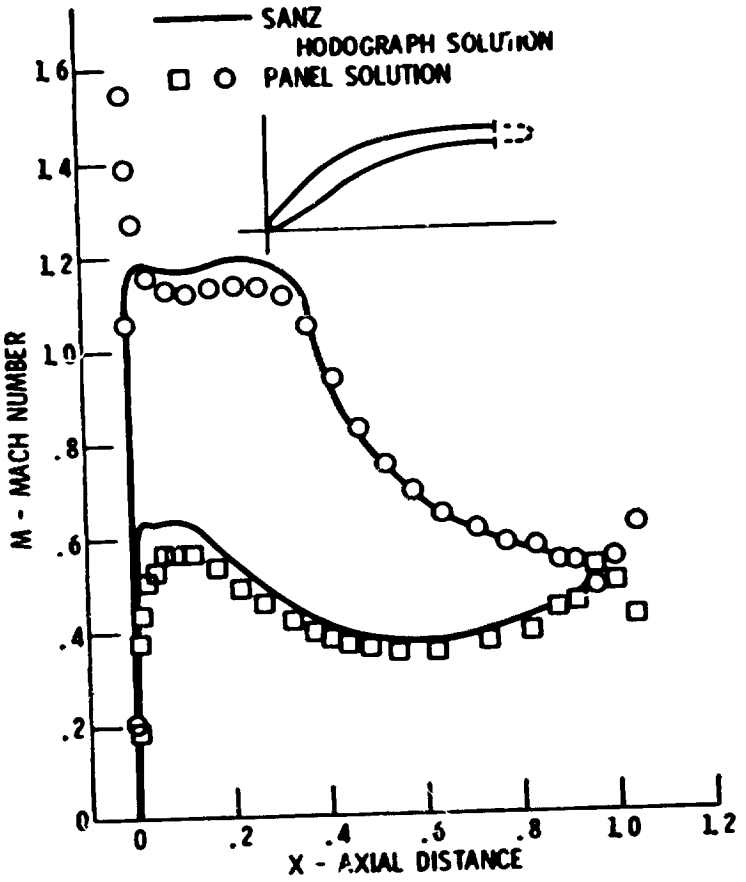

Figure 8. - Supercritical compressor stator.